International Journal of Pharmaceutics 389 (2010) 32–40

Contents lists available at ScienceDirect

International Journal of Pharmaceutics

journal homepage: www.elsevier.com/locate/ijpharm

Interaction dynamics of hypericin with low-density lipoproteins and U87-MG cells

Veronika Huntosova[a,b], Luis Alvarez[a], Lenka Bryndzova[b], Zuzana Nadova[b], Daniel Jancura[b], Luboslava Buriankova[b], Stéphanie Bonneau[a], Daniel Brault[a], Pavol Miskovsky[b,c,**], Franck Sureau[a,*]

[a] ANBioPhi, CNRS-FRE 3207, Pierre & Marie Curie University, Paris, France
[b] Department of Biophysics, University of Pavol Josef Safarik, Kosice, Slovak Republic
[c] International Laser Center, Bratislava, Slovak Republic

ARTICLE INFO

Article history:
Received 19 September 2009
Received in revised form 5 January 2010
Accepted 9 January 2010
Available online 18 January 2010

Keywords:
Hypericin
Low-density lipoproteins
Molecular interaction
Frequency domain fluorescence lifetime microspectrometry
Förster resonant energy transfer (FRET)
Photo dynamic therapy (PDT)

ABSTRACT

The natural photosensitizer hypericin exhibits potent properties for tumor diagnosis and photodynamic therapy. Fluorescent properties of hypericin along with various technical approaches have been used for dynamic studies of its interaction with low-density lipoprotein and U87 glioma cells. Evidences for hypericin release from low-density lipoprotein towards cells plasmatic membrane are addressed. Subsequent subcellular bulk flow redistribution leading to non-specific staining of intracellular membranes compartment were observed within cells. It was shown, that monomers of hypericin are the only redistributive forms. Increasing concentration of hypericin leads to the formation of non-fluorescent aggregates within low-density lipoprotein as well as within the U87 cells, and can preclude its photosensitizing activities. However, the aggregation process can only account for a part of the observed emission decrease. As shown by the excited state lifetime measurements, this fluorescence quenching actually results from a combination of aggregation process and energy transfer from monomers to aggregates. In all experiments, hydrophobic character of hypericin appears as the driving force of its redistribution process.

1. Introduction

Hypericin (Hyp) is a natural photosensitizer characterized by high singlet oxygen production (Olivo et al., 2006; Cole et al., 2008; Higuchi et al., 2008; Kacerovská et al., 2008). Its specific accumulation in tumor cells can be used for photo-diagnosis of early epithelial cancer (Sim et al., 2005; Fu et al., 2007; Kah et al., 2008; Ritz et al., 2008a). These properties together with minimal dark toxicity, and high clearance rate from the host body make Hyp a promising agent for PDT of cancer (Falk, 1999; Agostinis et al., 2002; Miskovsky, 2002; Kiesslich et al., 2006).

As expected from its molecular structure (Fig. 1), Hyp is a highly hydrophobic compound that forms non-fluorescent aggregates in aqueous solution. However absorption and fluorescence emission spectra of Hyp monomer can be observed after binding with various biological macromolecules (Das et al., 1999; Falk, 1999; Petrich, 2000; Miskovsky et al., 2001; Agostinis et al., 2002; Miskovsky, 2002; Kiesslich et al., 2006). Formation of reactive oxygen species (ROS) can only be obtained from its monomeric form (Senthil et al., 1992; Guedes and Erikson, 2005; Gbur et al., 2008, 2009). The very short lifetimes of ROS limit their diffusion through the cells. Consequently, the intracellular biological target and subsequent photo-induced cell death pathways (apoptotic or necrotic) are closely related to the subcellular localization of Hyp as well as to its monomers–aggregates balance. In this view, the intravascular transport of Hyp by LDLs and subsequent cellular uptake processes should be taken in consideration.

LDL is known as the main carrier of cholesterol in the human circulation system. It can be characterized as a spherical particle of 22 nm in diameter having three different regions. The outer surface layer, which consists of phospholipids molecules with a single apoB-100 protein; the core of LDL, which is enriched with triglycerides and cholesterol esters and an interfacial region between these two (Hevonoja et al., 2000). Due to the overexpression of specific receptors in many types of transformed cells (Brown and Goldstein, 1976; Vitols et al., 1992) LDL could play a key role in the targeted delivery of hydrophobic and/or amphiphilic photosensitizers to tumor cells for PDT (Jori, 1996; Reddi, 1997; Konan et al., 2002; Derycke and de Witte, 2004; Sherman et al., 2004).

Abbreviations: Hyp, hypericin; apoB-100, apolipoprotein B 100; DMSO, dimethyl-sulfoxide; FBS, fetal bovine serum; FRET, Fluorescence or Förster Resonant Energy Transfer; LDL, low-density lipoprotein; PDT, photodynamic therapy; pts, photosensitizer.

* Corresponding author at: ANBioPhi, genopole campus 1, 5 rue H. Desbruères, 91030 Evry Cedex, France. Tel.: +33 1 69874354; fax: +33 1 69874360.
** Corresponding author at: Department of Biophysics, University of Pavol Josef Safarik, Kosice, Slovak Republic.
E-mail addresses: pavol.miskovsky@upjs.sk (P. Miskovsky), franck.sureau@upmc.fr (F. Sureau).

0378-5173/$ – see front matter © 2010 Elsevier B.V. All rights reserved.
doi:10.1016/j.ijpharm.2010.01.010

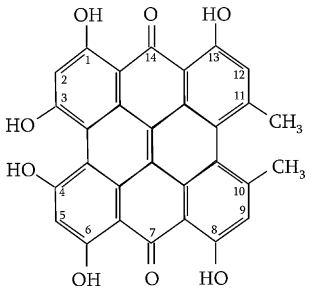

Fig. 1. Chemical structure of hypericin.

Previous investigations of Hyp interaction with LDL have shown non-specific binding of both its monomer and aggregate forms. Up to ~30 monomer molecules of Hyp can enter one LDL (Kascakova et al., 2005). Hyp are most likely embedded in the phospholipids shell of LDL close to the apoB-100 protein (Kascakova et al., 2008; Lajos et al., 2008; Mukherjee et al., 2008) and cholesterol has recently been identified as the key determinant of the observed selectivity of Hyp in model membrane systems (Ho et al., 2009). Upon increasing the Hyp concentration, the fluorescence quantum yield is dramatically decreased, suggesting most likely self-quenching of the aggregated form. It was shown that mixing of photosensitizers with LDL before in vivo administration led to a better delivery to target tissues and to an improved photodynamic efficacy (Korbelik, 1992, 1993; Chowdhury et al., 2003). Consistently, we have shown that over expression of LDL receptors leads to an increased accumulation of Hyp within U87 glioma cells (Kascakova et al., 2008). Therefore, the question is; what is the importance of the in vivo plasmatic transport of Hyp by LDL on the cellular uptake process and on its subsequent subcellular distribution. Does it enter cells through the endocytosis pathway of LDL or might the release of Hyp from LDL towards cellular membrane – prior to LDL endocytosis – be the main process? In this view, steady-state and kinetic studies of LDL–Hyp interaction were performed in using the fluorescence properties of Hyp.

2. Materials and methods

2.1. Chemicals

Hyp, LDL and LDL-bodipy (LDL_b) were all purchased from Gibco-Invitrogen, France.

2.2. Cell culture

The U87-MG human glioma cells were grown in Dulbecco's modified Eagle's medium (D-MEM) containing L-glutamine (862 mg L^{-1}), sodium pyruvate (110 mg L^{-1}), glucose (4500 mg L^{-1}), streptomycin (50 μg mL^{-1}), penicillin (50 μg mL^{-1}) and supplemented with 10% fetal bovine serum (FBS) or serum substitute 2% Ultroser G (Pall Corporation, France), in the presence of 5% CO_2 humified atmosphere at 37 °C. For all experiment cells were incubated in dark condition. All chemicals were obtained from Gibco-Invitrogen. For all cellular experiments, final content of DMSO was less than 1%.

2.3. Fluorescence spectroscopy

Interaction studies of hyp with LDL were performed in PBS pH 7.4. Solution of 10^{-8} M LDL was first prepared. Hyp was then added to reach different concentration ratio (from 3:1 up to 300:1) and samples were stabilized for 5 h. Fluorescence of Hyp was collected at 598 nm with an excitation at 515 nm in using a Shimadzu RF-5301 PC fluorimeter (Kyoto, Japan).

2.4. Stopped-flow measurements

Kinetic measurements of the redistribution of Hyp from [Hyp–LDL] saturated complexes towards free LDL were performed on a stopped-flow apparatus (Applied Photophysics, Leatherhead, UK) with a mixing time of 1.2 ms. The excitation light provided by a 150 W Xenon short-arc lamp was set at 550 nm. The fluorescence of the solution was collected above 600 nm using a low-cut filter (Oriel 51312, Stratford, CT). The signal was fed to a RISC workstation (Acorn Computers Limited, Cambridge, UK). Data were fitted in using the software from Applied Photophysics. The Levenberg–Marquard algorithm was used for non-linear curve fitting.

2.5. Flow-cytometric assay

U87-MG cells were first incubated for 6 h with different Hyp concentration (2.5–18.75 × 10^{-6} M), then washed by PBS, treated with EDTA/Trypsin and resuspended in 0.5 ml of PBS. Intracellular Hyp fluorescence was then determined over 10^5 events in using a Coulter Elite flow cytometer with a 488 nm laser excitation (Fl_3 channel detection, λ_{em} > 590 nm).

After measurement cells were centrifuged, disrupted with 5% SDS solution and subsequently diluted in 100% DMSO (final percentage 90%). Hyp fluorescence was then collected at 601 nm using 488 nm excitation wavelength.

2.6. Flow-cytometric assay of cellular uptake of hypericin

Cells were preincubated for 1 day in 2% Ultroser G medium. Hyp (5 × 10^{-7} M) or [Hyp–LDL] complexes (20:1, 200:1) were then added for different incubation time (1–24 h).

2.7. Fluorescence microscopy

Hyp (4 × 10^{-7} M) was gently mixed with LDL_b (2 × 10^{-8}) in PBS buffer (pH 7.4) and stabilized for 3 h in dark condition. U87-MG cells were first incubated for 1 day with 2% Ultroser G medium in 35 × 10 mm^2 Petri dishes. [Hyp–LDL_b] (20:1) complex was then added to cells for 1, 3 or 6 h before observation on an Optiphot-2 epifluorescence microscope equipped with a Nipkow wheel coaxial–confocal attachment (Technical Instrument, CA, USA). Fluorescence images were taken by using water-immersion objective (Zeiss Neofluar, X63, N.A. 1.2), TE cooled CCD Micromax camera (Princeton Instruments, NJ, USA) and standard filters system: FITC filter set (λ_{exc} = 450–490 nm, λ_{em} = 520–570 nm) or rhodamine filter set (λ_{exc} = 530–560 nm, λ_{em} > 600 nm). Exposure time was set to 5 s. Image processing was performed by IPLab software (Scanalytics, MD, USA).

2.8. Frequency domain fluorescence lifetime microspectrometry experiment

Our original fluorescent confocal microscope set-up enables concomitants spectroscopic and excited state lifetime measurements of the fluorescence emission signal. Frequency domain phase-modulation method used for lifetime determination appears to be particularly appropriate for rapid and non-invasive measurements on single living cells (Kocisova et al., 2003). Precise description of the set-up has already been published (Praus et al., 2007). Briefly, the 50 mW output laser diode module (LDM 442.50.A350 from Omicron) is used for excitation at 442 nm. Modulation frequencies are ranging from 10 to 200 MHz. A Zeiss UMSP-80

confocal epifluorescence upright microscope is used with a high numerical aperture water-immersion 63× magnification objective (Zeiss Neofluar, N.A. 1.2). A Jobin Yvon HR640 monochromator is used for dispersion of the fluorescence signal (10 nm/mm). Thus a 350 nm spectral region can be focused on the intensified digital CCD camera (Lambert Instruments, Roden, Netherlands) is used for detection.

A control unit drives the frequency and amplitude values of the RF modulation signals delivered by two synthesizers (model 2025 from IFR, Hertfordshire, UK) to the diode laser light source and to the image intensifier of the camera, respectively. It also induced precise phase shifts between the output signals of both synthesizers. The LIFLIM software (Lambert Instruments) is used for experimental data acquisition. Data processing for lifetime determination are performed in using global fitting procedure with Levenberg–Marquard algorithm. The most severe limit for the emission intensity is set by photobleaching in the sample (Hoebe et al., 2007). Hence, the 50 mW output power of the laser diode module is first attenuated (from 1/100 to 1/10.000) by interposition on the excitation pathway of neutral optical density filter. Further attenuations, through optics of the excitation pathway (lens, mirrors, interferential filter, and semi-transparent slide), lead to a measurable excitation power of only 0.1–1 μW at the sample level.

3. Results and discussion

3.1. Dynamic studies of Hyp–LDL interaction

The basic fluorescence spectroscopic study of Hyp interaction with LDL has already been described in our previous studies (Kascakova et al., 2005; Mukherjee et al., 2008). The concentration dependence of Hyp steady-state fluorescence emission in the presence of LDLs was monitored (Kascakova et al., 2005) and result of a similar experiment is given here (Fig. 2). While increasing the number of Hyp molecules per LDL molecule, a saturation effect of the fluorescence intensity is first observed, followed by a drastic decrease of the signal for higher ratios ($R > 50$). Above 150 molecules of Hyp per LDL, Hyp fluorescence even appears to be totally quenched. Self-quenching of aggregated Hyp has first been suggested to account for this observation (Kascakova et al., 2005). In order to get a better knowledge of what happens at high

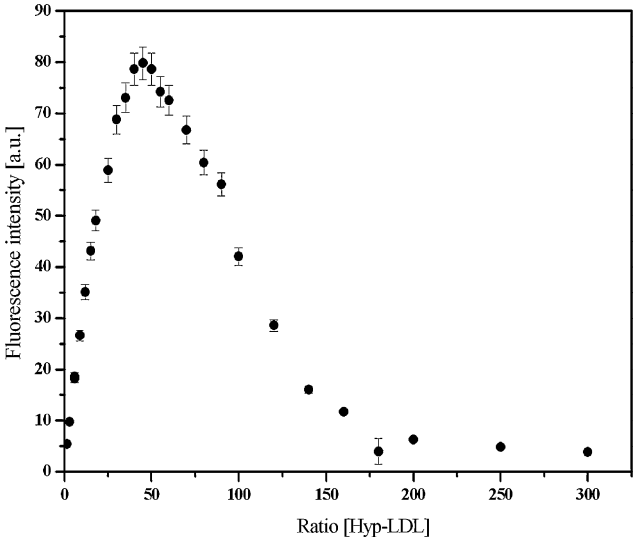

Fig. 2. Fluorescence intensity of increasing quantities of hypericin obtained after 5 h stabilization with 10^{-8} M LDLs solutions. The corresponding ratio R is given as the average number of hypericin molecules per one LDL molecule. Number of duplicate experiments: 3.

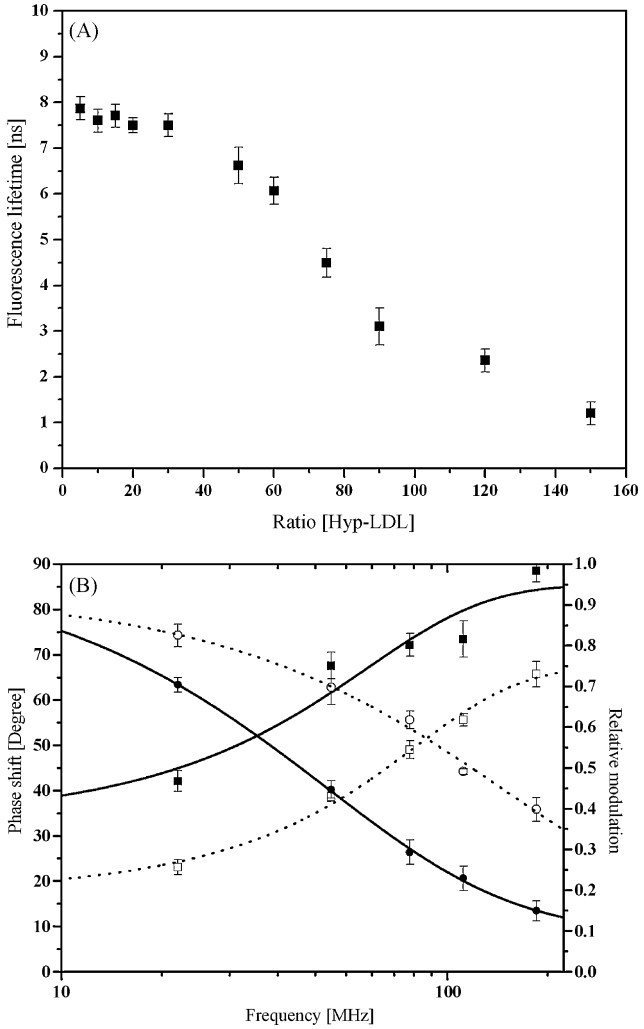

Fig. 3. (A) Dependence of the fluorescence lifetime of Hyp in LDL is given as a function of the ratio R (see Fig. 2). All data point measurements were performed with a fixed 4 μM Hyp concentration. Number of duplicate experiments: 2. (B) Illustration of the frequency response: Phase shift (squares) and relative modulation (circles) are given for Hyp in the presence of LDL in concentration ratio 30:1 (solid symbols) and 90:1 (open symbols). Solid and dotted lines correspond to the calculated fits for a single lifetime component analysis.

concentration ratio and to know if there is still some monomer form of Hyp useful for latest PDT application, frequency domain fluorescence lifetime's measurements of Hyp–LDL complex have then been performed at different ratio to better understand the observed fluorescence extinction process (Fig. 3A and B). The fluorescence lifetime is a very sensitive parameter of a fluorophore that can give evidences of specific interactions in excited state. Moreover it does not depend of its concentration. Results obtained with LDL give evidences that for low ratio <30:1 Hyp persist in the monomer form since the lifetime of Hyp remains the same for all concentration ratios. Higher concentration ratio of Hyp within LDL leads to a clear decrease of the Hyp fluorescence lifetime. Such result cannot be interpreted only by some non-fluorescent Hyp aggregates formation. However, taking into account the formation of Hyp aggregates for such ratio, this fluorescence lifetime decrease could be explain by the occurrence of intermolecular FRET from the monomer form towards non-fluorescent aggregate forms (Chen et al., 2001). Thus fluorescence lifetime measurements give evidences that even for high Hyp:LDL molecular ratio, part of the Hyp molecules are still under monomer form but that their fluorescence is quenched by some non-radiative Förster Reso-

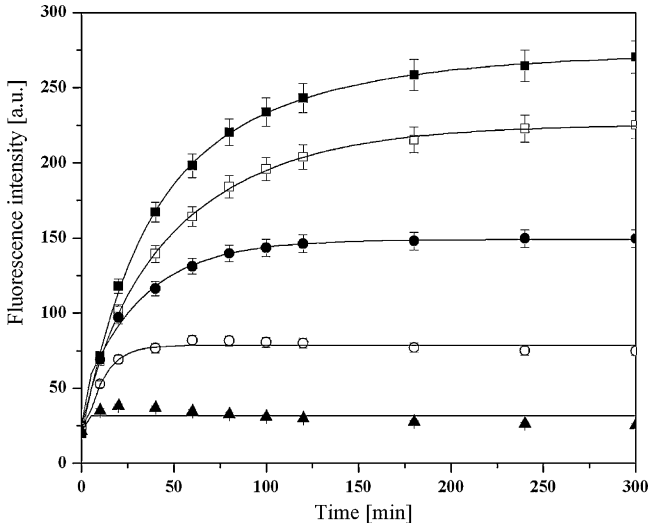

Fig. 4. Fluorescence intensity of Hyp/LDL complex after mixing of Hyp/LDL = 200/1 with appropriate amount of LDL in order to reach a final Hyp/LDL ratio of 10, 30, 60, 100, 150, respectively. Solid lines correspond to mono-exponential fits. Number of duplicate experiments: 3.

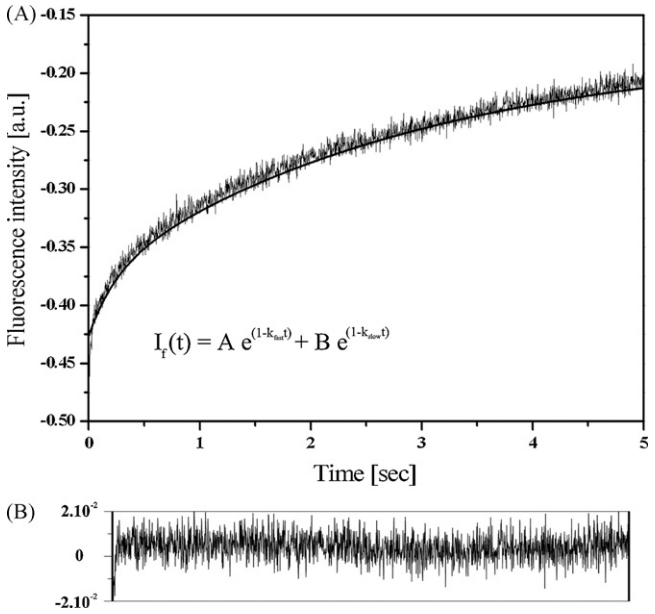

Fig. 5. (A) Fluorescence recovery of Hyp obtained after fast mixing (stopped-flow experiments) of 10^{-8} M Hyp–LDL saturated complex (R = 165) with 10^{-8} M free Hyp–LDL. Solid line corresponds to the theoretical bi-exponential fit. Number of duplicate experiments: 10. (B) Residual weight obtained with the bi-exponential fit of the experimental data.

nant Energy Transfer (FRET) toward the non-fluorescent aggregate form.

LDL have further been chosen as a model system for the investigation of Hyp transfer between lipid containing structures since

Table 1
Numerical values, of the bi-exponential fit, obtained after fast mixing of 10^{-8} M Hyp–LDL saturated complex solution (R = 165) with respectively 10^{-8} M (1:1), 2×10^{-8} M (2:1), and 4×10^{-8} M (4:1) free Hyp–LDLs solutions.

LDL/[Hyp–LDL]	A	k_{fast}	B	k_{slow}
1:1	0.0257	3.60	0.135	0.333
2:1	0.0632	4.67	0.195	0.326
4:1	0.0802	7.08	0.238	0.350

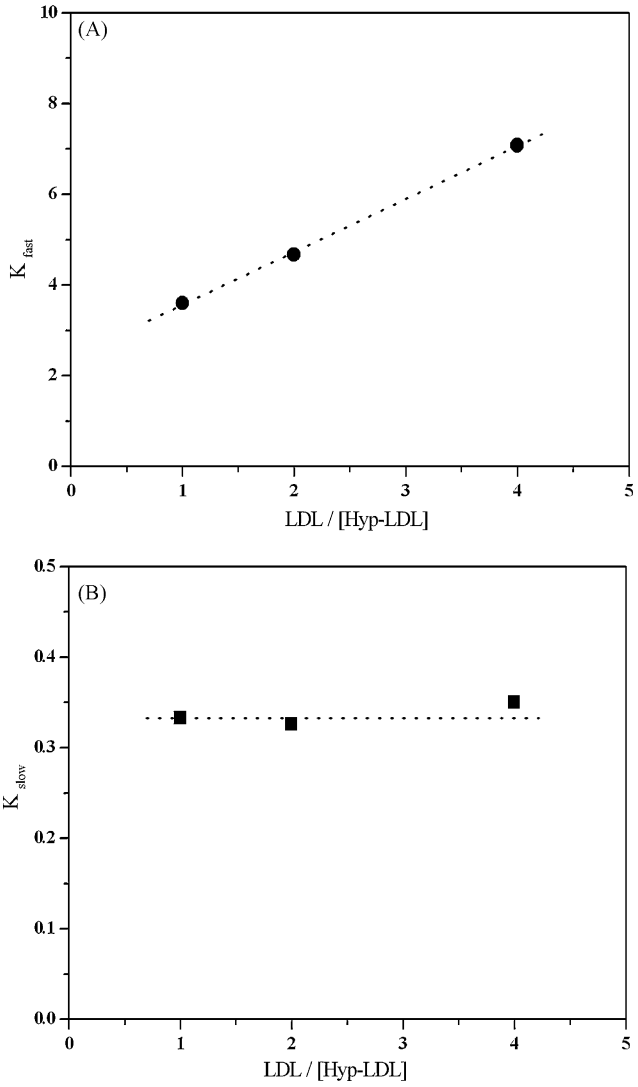

Fig. 6. (A) Evolution of the fast kinetic constant (k_{fast}) is given as a function of the concentration ratio of Hyp free LDL over Hyp–LDL saturated complex (correlation coefficient for the linear fit: 0.99). (B) Evolution of the slow kinetic constant (k_{slow}) is given as a function of the concentration ratio of Hyp free LDL over Hyp–LDL saturated complex (correlation coefficient for the constant fit: 0.81).

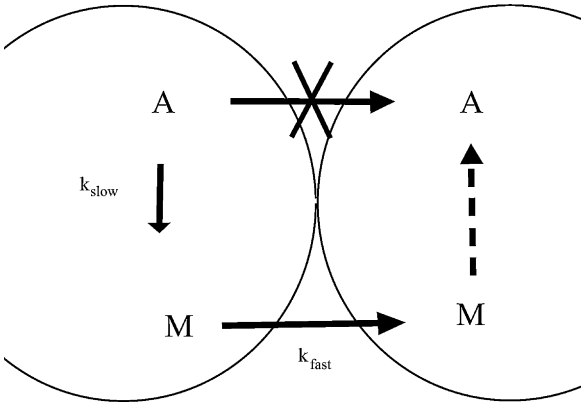

Fig. 7. Proposed scheme model for dynamic exchange of Hyp from saturated toward free LDLs.

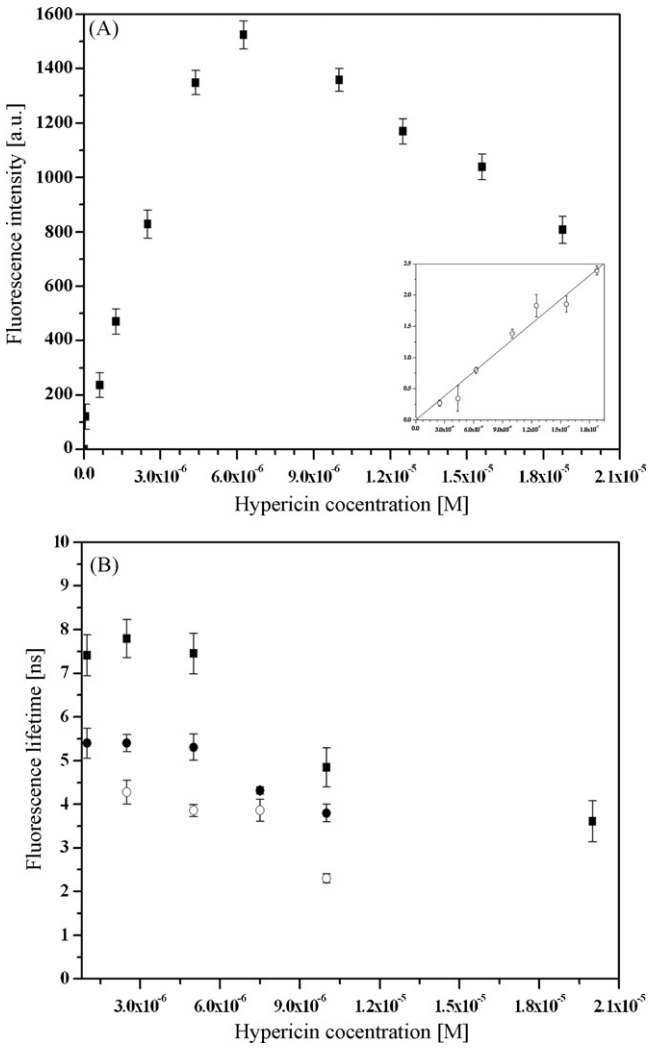

Fig. 8. (A) Fluorescence intensity obtained from cells after 6 h incubation with increasing Hyp concentration. *Insert*: corresponding fluorescence intensity observed after cells lyses and resuspension in DMSO. Number of duplicate experiments: 2. (B) Fluorescence lifetime obtained on single cells after 6 (solid square), 24 (solid circle), 48 (open circle) h incubation, with increasing Hyp concentration. Number of duplicate experiments: 2.

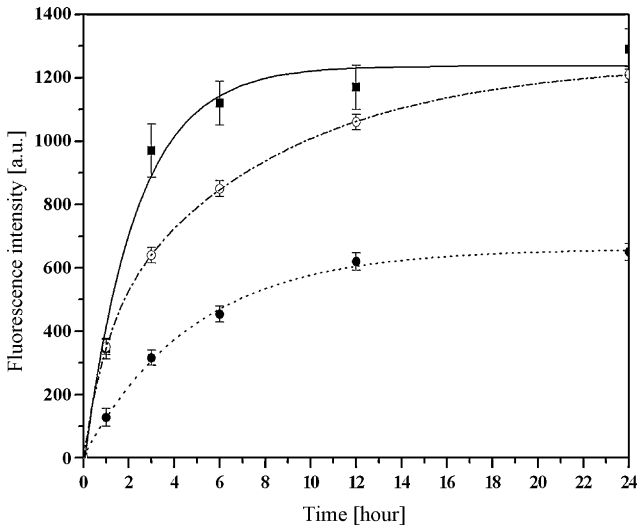

Fig. 9. Kinetics of cellular uptake for U87 cells incubated with 500 nM Hyp previously solved in DMSO (solid squares) in LDLs 200:1 (open circles) or in LDLs 20:1 (solid circles). Lines correspond to mono-exponential fits. Number of duplicate experiments: 2.

the almost total extinction of the fluorescence observed for very high Hyp–LDL ratio can be used for kinetics study of the transfer of Hyp molecules between LDL particles. Hence, time evolution of the fluorescence intensity after mixing of non-fluorescent LDL–Hyp saturated complex with Hyp free LDL have been obtained in using both classical spectroscopy and stopped-flow experiments (see Section 2). In classical spectroscopy experiments, the saturated complex (Hyp/LDL 200:1) was mixed in cuvette with adequate amounts of free LDL in order to reach specific Hyp/LDL final ratio ranging from 10 to 150 (Fig. 4). For each final ratio, an increase of the total intensity of Hyp fluorescence was observed. It gives evidence that aggregates of Hyp molecules are transferred from the Hyp/LDL (200:1) complex to free LDL particles where they are monomerized. This experiment clearly showed that molecules of Hyp can be transferred from one lipids containing macromolecule to another. Short-time evolution of the Hyp fluorescence recovery has then been monitored after fast mixing (1.2 ms) in using stopped-flow equipment. This short-time fluorescence recovery follows a bi-exponential function characterized by a fast (k_{fast}) and a slow (k_{slow}) constant (Fig. 5). These two constants have been measured in mixing different quantity of free LDL with a fix quantity of saturated complex (i.e., 1 to 1, 2 to 1, 4 to 1, see Table 1). The fast constant k_{fast} is clearly dependent on the quantity of free LDL mixed with the saturated Hyp–LDL complex, while the slow constant k_{slow} remains unchanged whatever the LDL/[LDL–Hyp] ratio (i.e., whatever the quantity of free LDL added). Moreover, as shown in Fig. 6A, k_{fast} appears directly proportional to the free LDL to saturated complex ratio. Thus free LDL concentration appears as the limited step for this fast transfer and it can be concluded that the mechanism for the transfer of Hyp monomer is governed by simple equilibrium diffusion during collision between LDLs. On the other side, k_{slow} remains the same whatever the free LDL to saturated complex ratio (Fig. 6B). Thus transition from the aggregate to the monomer form within LDLs appears as the limiting step for the slow transfer. All together, these results are interpreted by the fact that transfer between LDL only occurs for the monomer form of Hyp. Hence some schematic model for dynamic exchange of Hyp from saturated toward free LDLs is proposed in Fig. 7.

3.2. Determination of the intracellular Hyp concentration

So we have shown that the aggregate non-active form of Hyp can saturate LDL, which could be useful for safe drug delivery. But what is about intracellular Hyp? Further experiments have been performed at the cellular level in order to get an answer. The fluorescence intensity of Hyp inside U87-MG cells as a function of Hyp concentration is presented in Fig. 8A. Cells were incubated with Hyp for 6 h with increasing Hyp concentration and the total fluorescence of Hyp, accumulated inside cells, was then determined by flow cytometry. The fluorescence intensity increases up to a concentration of 6×10^{-6} M and beyond this value fluorescence

Fig. 10. (A) Microscopic fluorescence image of U87 cells incubated in presence of the complex [LDL_b–Hyp] 20:1 for 1 h (first row), for 3 h (second row) and 6 h (third row). Left column is corresponding to the green fluorescence emission of LDL_b and right column to the red fluorescence emission of Hyp. Number of duplicate experiments: 2. (B) Corresponding intracellular fluorescence spectrum obtained after 3 h incubation with the complex [LDL_b–Hyp] 20:1 (the right band (c) peaking at 604 nm corresponds to the fluorescence of Hyp, the central band (b) peaking at 525 nm corresponds to the fluorescence of LDL_b and the sharp band (a) at left corresponds to the elastic scattering of the excitation).

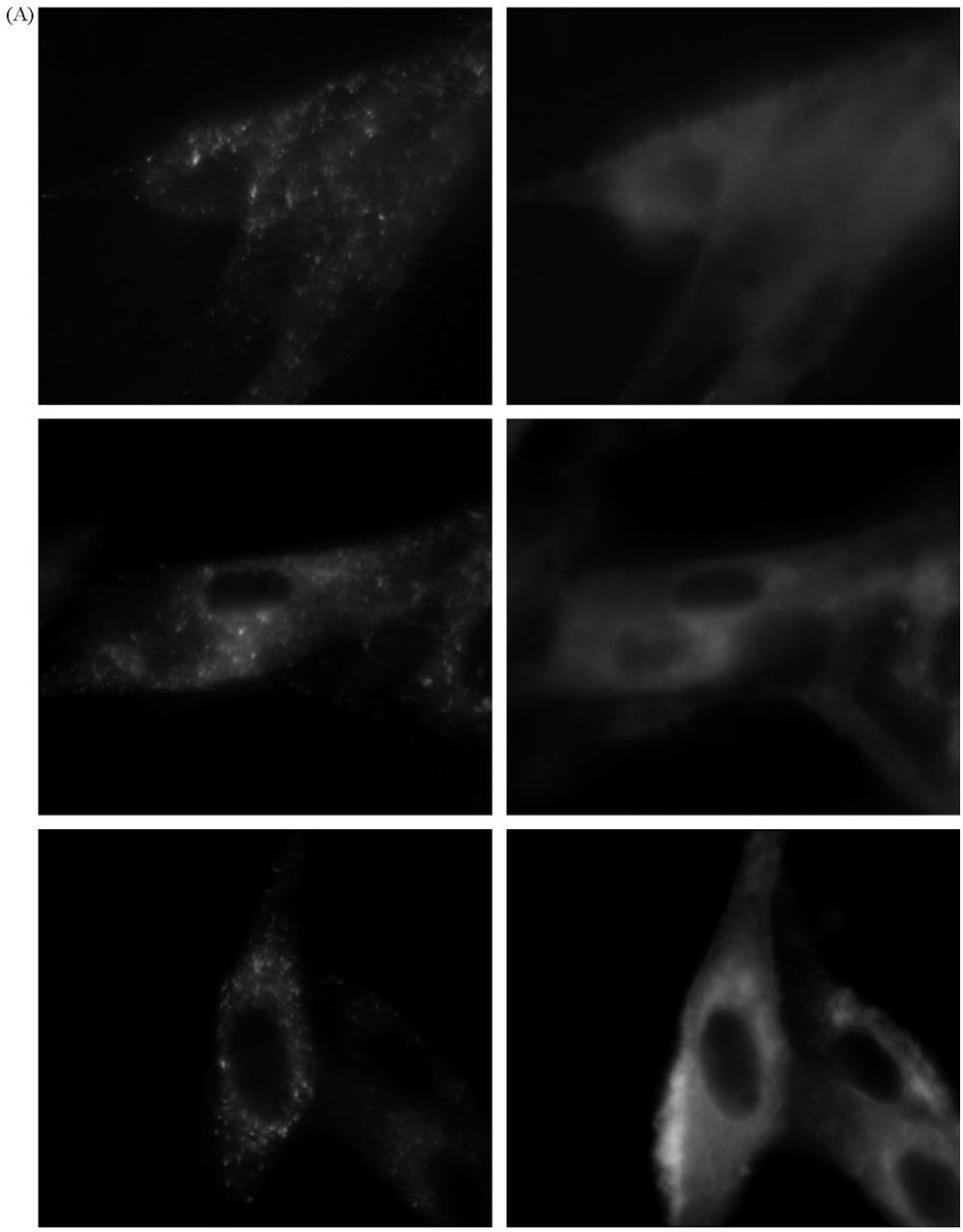
(A)

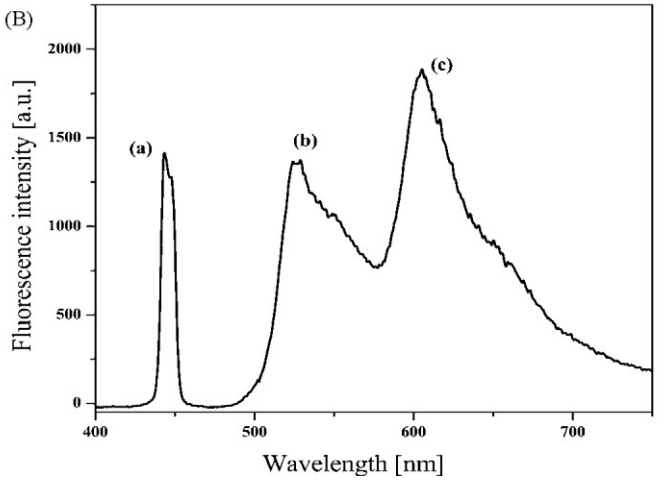
(B)
Fluorescence intensity [a.u.]
Wavelength [nm]
(a)
(b)
(c)
0
500
1000
1500
2000
400
500
600
700

moderately decreases. The course of this dependence is qualitatively similar to that observed for Hyp accumulation inside LDL particles (Fig. 2 and Kascakova et al., 2005). However, the real intracellular concentration of Hyp, which was determined by the measurement of fluorescence intensity from the cell lysate solubilized in DMSO (this experimental procedure guarantees that all Hyp molecules localized in the cells are in monomeric — fluorescence state) is still directly proportional to the total concentration of Hyp in the cultivation medium (insert Fig. 8A). This last results suggests that for high intracellular Hyp concentrations not all accumulated Hyp can be detected by steady-state fluorescence spectroscopy or microscopy. In other words, the fluorescence intensity of Hyp accumulated inside cells does not always corresponds to the total cellular concentration of the drug. Thus high intracellular concentration clearly leads to fluorescent quenching as the consequence of Hyp aggregation. In such a situation, the measurement of fluorescence lifetime of Hyp can provide useful informations about the real concentration of fluorescence molecules inside the cells. The dependence of the fluorescence lifetime of Hyp localized inside cells on Hyp concentration is shown in Fig. 8B. For the incubation time 6 h, the value of the lifetime is around 7.4 ns and remains constant up to a concentration of 1×10^{-5} M. This value is in a very good agreement with our previous results (Gbur et al., 2009) and other published data (Lenci et al., 1995) about the fluorescence properties of the monomer form of Hyp in lipid environment. The further increase of Hyp concentration leads to a shortening of its fluorescence lifetime. The course of this dependence is qualitatively similar to that observed for Hyp accumulation inside LDL particles (Fig. 3A). This observation confirms the existence of the self-quenching of the single excited state of Hyp inside the cells at high Hyp concentrations. Thus, above some critical intracellular concentration both fluorescence intensity and fluorescence lifetime of Hyp are decreasing. Similar results have been obtained with isolated mitochondria (data not shown). It should be noted that initial extracellular concentration of Hyp that is necessary to reach such intracellular critical concentration is tightly dependent on the cellular incubation time since after 24 and 48 h, fluorescence lifetimes of Hyp are already decreasing to 6.0 and 5.5 ns, respectively even for the lowest extracellular concentration (Fig. 8B). Thus, the combination of steady-state and time-resolved fluorescence spectroscopies can only provide correct estimation of the intracellular concentration of this drug.

3.3. The mechanism of intracellular uptake of Hyp

It is known that upon administration into the bloodstream Hyp associates with serum proteins, mainly with LDL (Chen et al., 2001). The question is what is the importance of the in vivo plasmatic transport of Hyp by LDL, its natural carriers, on the cellular uptake and accumulation processes and on the subsequent subcellular distribution. In our previous work, we have already shown that higher number of LDL receptors on the surface of U87-MG cells leads to a higher intracellular uptake of Hyp in the presence of LDL (Kascakova et al., 2008). We have proposed that LDL receptor pathway play an important role in the delivery and accumulation of Hyp into the cells. However, the question about the mode of the cellular uptake of Hyp is still not completely resolved. More specifically, does Hyp enter cells through the endocytosis pathway of LDL or does Hyp release from LDL towards cellular membrane prior to LDL endocytosis happen? In this view, the influence of the Hyp/LDL ratio on the kinetic of the cellular uptake of Hyp was studied. Different samples of U87-MG cells were incubated in the presence of a constant concentration of Hyp (500 nM) in D-MEM solutions that were previously prepared by solubilization with either DMSO (0.5%), or within LDL ($R = 200$ and $R = 20$). Results of the experiments are presented in Fig. 9. Interestingly, quite similar results

Table 2
Fluorescence lifetimes of LDL_b.

Fluorescence lifetime of LDL_b	In solution	In cells
LDL_b in the absence of hypericin	2.3 ± 0.1 ns	3.4 ± 0.1 ns
LDL_b in the presence of hypericin	1.1 ± 0.1 ns	3.5 ± 0.1 ns

are obtained both for Hyp overloaded in LDL ($R = 200$) and for Hyp merely solved with DMSO (final concentration of DMSO was 0.5%). Thus, the non-fluorescent Hyp aggregates initially embedded in LDL lead to the same time course of the fluorescence intensity than that observed for Hyp alone. This observation suggests that Hyp can be released from overloaded LDL particles and incorporated as monomers into cellular membrane exactly in the same way than those previously observed between LDL molecules. Moreover, it is in agreement with the assumption that photosensitizers, which are hydrophobic and have two or less negative charges, can diffuse across the plasma membrane, and then relocate to other intracellular membranes (Castano et al., 2004). On the other side, cellular uptake of Hyp appears to be lower in the case of Hyp/LDL = 20:1 complex in comparison with the Hyp:LDL = 200:1 one. Taking into account the finite number of LDL receptors on the cellular cytoplasmatic membrane, this observation could be explained by the fact that in the first case up to 200 Hyp molecules can be delivered to the cell through each LDL receptor while only 20 of them can be delivered in the second case. Moreover, this result is consistent with some passive redistribution process for which amplitude is directly related to concentration gradient between LDL and cell membrane compartment. Hence balance between passive diffusion and solubility on one side and active membrane transport pathway (such as endocytosis or pinocytosis) on the other side probably depends on the Hyp/LDL ratio. As was recently pointed out (Ho et al., 2009), this aspect is of a great importance since intracellular localization of Hyp plays an essential role in its phototoxic activity. Mitochondrial localization leads to apoptotic cell death (Ali and Olivo, 2002), while lysosomal localization delays the apoptotic process and predisposes cells to necrosis (Kessel et al., 1997; Moor, 2000). In using bodipy-fluorescent labeled LDL (LDL_b), fluorescence imaging experiments and fluorescence lifetime measurements were realized in order to get further evidence about Hyp release from LDL towards cell membrane. If the cellular uptake of Hyp is realized mainly through the LDL pathway, then the initial subcellular localization of Hyp should be lysosomes. As shown in Fig. 10A, 1 h after incubation, the intracellular Hyp fluorescence appears to be non-specifically localized all over the cytosolic compartments, while some ponctuate fluorescent pattern is observed for LDL_b, corresponding to the expected lysosomes specific staining following endocytosis process. For longer incubation times, LDL_b fluorescence pattern still remains the same, while Hyp fluorescence becomes more intense in the perinuclear region. This is in agreement with some recent published studies showing that subcellular localization of Hyp is dominantly in the endoplasmic reticulum and Golgi apparatus in glioblastoma cells (Agostinis et al., 2002; Ritz et al., 2008b). Fluorescent resonant energy transfer (FRET) from the bodipy-stained LDL to Hyp molecules can be used to give direct evidence of the formation of Hyp/LDL complex (Fig. 10B) (Chen et al., 2008). Such FRET is actually observed in an aqueous solution where the fluorescent lifetime of the LDL-bodipy marker, which is 2.3 ± 0.1 ns in the absence of Hyp, is decreased to 1.1 ± 0.1 ns in the presence of Hyp (see Table 2). The fluorescence lifetime of the bodipy-LDL obtained from the cells incubated with Hyp–LDL_b complex (Hyp/LDL = 20:1) is not decreased when compared with the lifetime of the marker incubated alone with the cells. Thus, intracellular Hyp does not interact with LDL since FRET cannot be observed inside cells. All together, these results suggest that Hyp binding to

LDLs is very important for cellular targeting and could play a key role in the observed "in vivo" specific tumor accumulation but it does not affect the subcellular distribution of Hyp as compared to cells incubated with Hyp alone. Moreover, it should be noted that the kinetic of the cellular uptake process could be affected by the initial Hyp/LDL ratio.

4. Conclusion

In this work, dynamic studies gives clear evidences that the monomer form of Hyp which was already considered as the only photoactive form should also be considered as the only redistributive form while aggregate form should be considered as a monomer delivery delay form. However, the transport of Hyp under aggregate form in overloaded LDL (Hyp/LDL = 200:1) not only allows precluding the toxic photo-oxidation process of LDL prior to cellular uptake but also leads to an higher intracellular accumulation of the drugs when compared to results obtained for the same quantity of Hyp loaded within LDLs to a 10-fold lower ratio (Hyp/LDL = 20:1). Moreover the Hyp/LDL molar ratio could affect the subcellular distribution of Hyp: overloaded LDLs should favor the passive bulk flow diffusion process leading to non-specific membrane staining while underloaded LDLs (Hyp/LDL < 10:1) might favor the endocytosis pathway leading to lysosomal staining as previously observed (Kascakova et al., 2008).

In a more general way, we also provide clear evidence that for the determination of the real intracellular concentration of hydrophobic pts, like Hyp, it is not sufficient to measure the fluorescence intensity of the molecule. The combination of steady-state and time-resolved fluorescence spectroscopies is the only way to reach correct estimation of the intracellular concentration of such fluorescence drugs. Hence, the fluorescence lifetime experiments appears to be a useful approach to determine the aggregate versus monomer balance in order to assess the real potential photo-induced biological activity of Hyp inside the cells.

Acknowledgements

This work was supported by the Slovak Research and Development Agency contracts No. APVV-0449-07 and APVV-LPP-0337-06, the Scientific Grant Agency of the Ministry of Education of Slovak Republic (grant VEGA-0164-09). The authors thank the Synchrotron SOLEIL for providing the detection system of the DISCO beamline.

References

Agostinis, P., Vantieghem, A., Merievede, W., de Witte, P., 2002. Hypericin in cancer treatment: more light on the way. Int. J. Biochem. Cell Biol. 34, 221–241.

Ali, S.M., Olivo, M., 2002. Bio-distribution and subcellular localization of hypericin and its role in PDT induced apoptosis in cancer cells. Int. J. Oncol. 21, 531–540.

Brown, M.S., Goldstein, J.L., 1976. Receptor mediated control of cholesterol metabolism. Science 191, 150–154.

Castano, A.P., Demidova, T.N., Hamblin, M.R., 2004. Mechanisms in photodynamic therapy: part one—photosensitizers, photochemistry and cellular localization. Photodiagn. Photodyn. Ther. 1, 279–293.

Chen, B., Xu, Y., Roskams, T., Delay, E., Agostinis, P., Vanderheede, J.R., de Witte, P., 2001. Efficacy of antitumoral photodynamic therapy with hypericin: relationship between biodistribution and photodynamic effects in the RIF-1 mouse tumor model. Int. J. Cancer 93, 275–282.

Chen, H., Kim, S., Li, L., Wang, S., Park, K., Cheng, J.X., 2008. Release of hydrophobic molecules from polymer micelles into cell membranes revealed by Förster resonance energy transfer imaging. Proc. Natl. Acad. Sci. U.S.A. 105, 6596–6601.

Chowdhury, R.K., Sharif, I., Chansarkar, N., Dolphin, D., Ratkay, L., Delaney, S., Meadows, H., 2003. Correlation of photosensitizer delivery to lipoproteins and efficacy in tumor and arthritis mouse models: comparison of lipid-based and Pluronic P123 formulations. J. Pharm. Pharm. Sci. 6, 198–204.

Cole, C.D., Liu, J.K., Sheng, X., Chin, S.S., Schmidt, M.H., Weiss, M.H., Couldwell, W.T., 2008. Hypericin-mediated photodynamic therapy of pituitary tumors: preclinical study in a GH4C1 rat tumor model. J. Neurooncol. 87, 255–261.

Das, K., Smirnov, A.V., Wen, J., Miskovsky, P., Petrich, J.W., 1999. Photophysics of hypericin and hypocrellin A in complex with subcellular components: interactions with human serum albumin. Photochem. Photobiol. 69, 633–645.

Derycke, A.N.L., de Witte, P., 2004. Liposomes for photodynamic therapy. Adv. Drug Deliv. Rev. 56, 17–30.

Falk, H., 1999. From the photosensitizer hypericin to the photoreceptor stenorin: the chemistry of phenanthroperylene quinines. Angew. Chem. Int. Ed. Engl. 38, 3116–3136.

Fu, C.Y., Ng, B.K., Razul, S.G., Chin, W.W., Tan, P.H., Lau, W.K., Olivo, M., 2007. Fluorescence detection of bladder cancer using urine cytology. Int. J. Oncol. 31, 525–530.

Gbur, P., Dedic, R., Jancura, D., Miskovsky, P., Hala, J., 2008. Time resolved luminescence and singlet oxygen formation under illumination of hypericin in acetone. J. Luminescence 128, 765–767.

Gbur, P., Dedic, R., Chorvat Jr., D., Miskovsky, P., Hala, J., Jancura, D., 2009. Time-resolved luminescence and singlet oxygen formation after illumination of the hypericin-low-density lipoprotein complex. Photochem. Photobiol. 85, 816–823.

Guedes, R.C., Erikson, L.A., 2005. Theoretical study of hypericin. J. Photochem. Photobiol. A Chem. 172, 293–299.

Hevonoja, T., Petikainen, M.O., Hyvonen, M.T., Kovanen, P.T., Ala-Korpela, M., 2000. Structure of low density lipoprotein (LDL) particles: basis for understanding molecular changes in modified LDL. Biochem. Biophys. Acta 1488, 189–210.

Higuchi, A., Yamada, H., Yamada, E., Jo, N., Matsumura, M., 2008. Hypericin inhibits pathological retinal neovascularization in a mouse model of oxygen-induced retinopathy. Mol. Vis. 14, 249–254.

Ho, Y.F., Wu, M.H., Cheng, B.H., Chen, Y.W., Shih, M.C., 2009. Lipid-mediated preferential localization of hypericin in lipid membranes. Biochim. Biophys. Acta 1788, 1287–1295.

Hoebe, R.A., Van Oven, C.H., Gadella Jr., T.W., Dhonukshe, P.B., Van Noorden, C.J., Manders, E.M., 2007. Controlled light-exposure microscopy reduces photobleaching and phototoxicity in fluorescence live-cell imaging. Nat. Biotechnol. 25, 249–253.

Jori, G., 1996. Tumour photosensitizers: approaches to enhance the selectivity and efficacy of photodynamic therapy. J. Photochem. Photobiol. B Biol. 36, 87–93.

Kacerovská, D., Pizinger, K., Majer, F., Smíd, F., 2008. Photodynamic therapy of nonmelanoma skin cancer with topical hypericum perforatum extract—a pilot study. Photochem. Photobiol. 84, 779–785.

Kah, J.C., Lau, W.K., Tan, P.H., Sheppard, C.J., Olivo, M., 2008. Endoscopic image analysis of photosensitizer fluorescence as a promising noninvasive approach for pathological grading of bladder cancer in situ. J. Biomed. Opt. 13, 054022.

Kascakova, S., Refregiers, M., Jancura, D., Sureau, F., Maurizot, J.C., Miskovsky, P., 2005. Fluorescence spectroscopic study of hypericin-photosensitized oxidation of low-density lipoproteins. Photochem. Photobiol. 81, 1395–1403.

Kascakova, S., Nadova, Z., Mateasik, A., Mikes, J., Huntosova, V., Refregiers, M., Sureau, F., Mauriziot, J.C., Miskovsky, P., Jancura, D., 2008. High level of low-density lipoprotein receptors enhance hypericin uptake by U-87 MG cells in the presence of LDL. Photochem. Photobiol. 84, 120–127.

Kessel, D., Luo, Y., Deng, Y., Chang, C.K., 1997. The role of subcellular location in initiation of apoptosis by photodynamic therapy. Photochem. Photobiol. 65, 422–425.

Kiesslich, T., Krammer, B., Plaetzer, K., 2006. Cellular mechanism and prospective applications of hypericin in photodynamic therapy. Curr. Med. Chem. 13, 2189–2204.

Kocisova, E., Sureau, F., Praus, P., Rosenberg, I., Stepanek, J., Turpin, P.Y., 2003. Monitoring of labeled antisense oligonucleotides within living cells by using a multifrequency phase/modulation approach for fluorescence lifetime measurements. J. Mol. Struct. 651–653, 115–122.

Konan, Y.N., Gurny, R., Alleman, E., 2002. State of the art in the delivery of photosensitizers for photodynamic therapy. J. Photochem. Photobiol. B Biol. 66, 89–106.

Korbelik, M., 1992. Low density lipoprotein receptor pathway in the delivery of photofrin: how much it is relevant for selective accumulation of the photosensitizers in tumors? J. Photochem. Photobiol. B Biol. 12, 107–109.

Korbelik, M., 1993. Cellular delivery and retention of photofrin II: role of plasma proteins in photosensitizer's clearance from cells. Photochem. Photobiol. 57, 846–850.

Lajos, G., Jancura, D., Miskovsky, P., Garcia-Ramos, J.V., Sanchez-Cortes, S., 2008. Surface-enhanced fluorescence and Raman scattering study of antitumoral drug hypericin: an effect of aggregation and self-spacing depending on pH. J. Phys. Chem. C 112, 12974–12980.

Lenci, F., Angelini, N., Ghetti, F., Sgarbosa, A., Losi, A., Vecli, A., 1995. Spectroscopic and photoacoustic studies of hypericin embedded in liposomes as a photoreceptor model. Photochem. Photobiol. 62, 199–204.

Miskovsky, P., Hritz, J., Sanchez-Cortes, S., Fabriciova, G., Ulicny, J., Chinsky, L., 2001. Interaction of hypericin with serum albumins: surface-enhanced Raman spectroscopy, resonance Raman spectroscopy and molecular modeling study. Photochem. Photobiol. 74, 172–183.

Miskovsky, P., 2002. Hypericin-a new antiviral and antitumor photosensitizer: mechanism of action and interaction with biological macromolecules. Curr. Drug Targets 3, 55–84.

Moor, A.C., 2000. Signaling pathway in cell death and survival after photodynamic therapy. J. Photochem. Photobiol. B 57, 1–13.

Mukherjee, P., Adhikary, R., Halder, M., Petrich, J.W., Miskovsky, P., 2008. Accumulation and interaction of hypericin in low-density lipoprotein—a photophysical study. Photochem. Photobiol. 84, 706–712.

Olivo, M., Du, H.Y., Bay, B.H., 2006. Hypericin lights up the way for the potential treatment of nasopharyngeal cancer by photodynamic therapy. Curr. Clin. Pharmacol. 1, 217–222.

Petrich, J.W., 2000. Excited-state intramolecular H-atom transfer in nearly symmetrical perylene quinines: hypericin, hypocrelin and their analogs. Int. Rev. Phys. Chem. 19, 479–500.

Praus, P., Kocisova, E., Stepanek, J., Seksek, O., Sureau, F., Turpin, P.Y., 2007. Advanced microfluorescence methods in monitoring intracellular uptake of "antisense" oligonucleotides. Curr. Org. Chem. 11, 515–527.

Reddi, E., 1997. Role of delivery vehicles for photosensitizers in the photodynamic therapy of tumors. J. Photochem. Photobiol. B Biol. 37, 189–195.

Ritz, R., Roser, F., Radomski, N., Strauss, W.S., Tatagiba, M., Gharabaghi, A., 2008a. Subcellular colocalization of hypericin with respect to endoplasmic reticulum and Golgi apparatus in glioblastoma cells. Anticancer Res. 28, 2033–2038.

Ritz, R., Müller, M., Dietz, K., Duffner, F., Bornemann, A., Roser, F., Tatagiba, M., 2008b. Hypericin uptake: a prognostic marker for survival in high-grade glioma. J. Clin. Neurosci. 15, 778–783.

Senthil, V., Longworth, J.W., Ghiron, C.A., Grossweiner, L.J., 1992. Photosensitization of aqueous model systems by hypericin. Biochim. Biophys. Acta 1115, 192–200.

Sherman, W.M., van Lier, J.E., Allen, C.M., 2004. Targeted photodynamic therapy via receptor mediated delivery systems. Adv. Drug Deliv. Rev. 56, 53–76.

Sim, H.G., Lau, W.K., Olivo, M., Tan, P.H., Cheng, C.W., 2005. Is photodynamic diagnosis using hypericin better than white-light cystoscopy for detecting superficial bladder carcinoma? BJU Int. 95, 1215–1218.

Vitols, S., Peterson, C., Larsson, O., Holm, P., Aberg, B., 1992. Elevated uptake of low-density lipoproteins by human cancer tissue in vivo. Cancer Res. 52, 6244–6247.